A Multiscale Simulation Approach for Diesel Particulate Filter Design Based on OpenFOAM and DexaSIM.

Johannes Leixnering MSc[1]
Bernhard Gschaider MSc[1]
Wilhelm Brandstätter Prof[2]
Ries Bouwman MSc[2]

[1] ICE Strömungsforschung GmbH, Hauptplatz 13, 8700 Leoben, Austria
[2] Montanuniversität Leoben, Franz-Josefstrasse 18, 8700 Leoben, Austria

Abstract

The majority of Diesel exhaust gas aftertreatment system design and development work is done experimentally by means of long and expensive engine bench tests.

The final system configuration is generally the product of a series of experimental “trial and error” operations. In order to shorten the development process, to reduce testing costs and to increase the durability of Diesel Particulate Filters (DPFs), multi-disciplinary simulation tools are needed to predict possible failures of the DPF.

Recently, several numerical models have been developed to simulate globally the soot loading capacity, the pressure drop evolution and the regeneration behaviour in ceramic wall-flow filters. Less effort has been devoted to the development of dedicated models for the simulation of the microstructural flow phenomena and thermo-mechanical behaviour of the filters.

This paper describes the development of a multi-physics software tool based on OpenFOAM embedded in the DexaSIM Graphical User Interface (GUI) which is able to handle the evolution of microstructural material properties and complex physical phenomena inside the filter material as well as response of complete filters under engine operating conditions.

The modelling approach hence builds on the multiscale link between microstructural evolution and specific macroscopic exhaust system features with the objective to achieve major improvements in material design and lifecycle assessment.

Introduction

During the last few years Diesel engines have shown a great potential in terms of performance, fuel economy and pollutant emissions, so that they are currently moving the major part of the European vehicle fleet. On the other hand, emission regulations are becoming more and more stringent and car manufacturers, as a consequence, have to find solutions to cope with the upcoming legislation.

Two possible methods are foreseen for lowering emissions; the first is to reduce the pollutant production during combustion and the second to purify the gases by filters and catalytic treatment in the engine exhaust system.

Diesel Particulate Filters (DPF)

In particular, the application of Diesel Particulate Filters (DPFs) demonstrated to be a good solution to abate particulate matter (PM) quantity to the required limits. The innovation in this field is not yet finished as the imposed limits evolve continuously and different combustion products (particle dimension, density, etc.) appear due to the introduction of new combustion concepts.

The design and development of exhaust gas aftertreatment systems today is done mostly experimentally by means of long and expensive engine bench tests. The final system configuration is generally the product of a series of experimental “trial and error” operations. Within this process, filter regeneration behaviour is the most critical event for the whole system since very high pressures (due to high soot accumulation) and temperatures can affect the complete filter which generally consists of filter substrate, catalytic coating, fibre mats and metal canning. However, each one of these components is difficult to investigate in detail. Especially the filter material can only be investigated to a minor degree after the experimental tests by destructive methods (burning, cutting). No detailed information on the soot deposition, the heat transfer and other typical phenomena inside the filter can be obtained with the experimental tools available.

In view of this it is no wonder that engine and exhaust system developers want to gain a deeper insight into the chemical and physical phenomena happening in DPFs during filter regeneration than obtainable on a pure experimental basis. In order to shorten the development process, to reduce testing costs and to increase the durability of DPFs, multi-disciplinary simulation tools are needed to predict possible failures of the DPF.

Already in recent years several numerical models have been developed to simulate globally the soot loading capacity, the pressure drop evolution and the regeneration behaviour in typical ceramic wall-flow filters [13, 19]. Less effort has been devoted to the development of dedicated models for the simulation of the *microstructural* thermo-mechanical behaviour of the ceramic filter at high temperature, to evaluate the resistance to thermal fatigue (crack formation and evolution), corrosion (ashes contact), substrates oxidation and filtration efficiency evolution (porosity and micro-cracks modifications).

Furthermore *macrostructural* properties of the filter and the mat in order to optimise the canning process and in service durability should be predicted by computer modelling. Among the mat failures to be foreseen, the vermiculite collapse at high temperature, the incomplete binder burning and the fibre erosion due to strong vibrations are the most important ones.

So far no modelling software in the Automotive industry is available, where the micro-structural evolution of filter material and the macroscopic behaviour of the complete engine exhaust system due to soot deposition/burn off and temperature induced stresses can be computed, let alone mesh generators of typical porous filter material.

Multiscale simulations

The need for engineering modelling tools to assist DPF and overall exhaust system design optimization already in the past has let to different approaches on the basis of 1D [15] and 3D [11] models. However, all of them are applied solely on a macroscopic level, where homogeneous porosities and measured permeabilities are used to model the effect of filter material on the exhaust gas flow. Without extensive experimental calibration the predictive capability of these models proved to be limited.

Only a few attempts [10, 16] are known to compute micro-structural flow phenomena in filters using the Lattice-Boltzmann-Method (LBM). The work thereby focussed on the computation of cold flow and particle deposition in porous media and not on heat transfer and chemical surface reactions due to inherent limitations of the LBM in this area.

Recently also the explicit coupling of 1D and 3D software [20] with respect to filter regeneration modelling was attempted. The approach showed certain problems. In particular the initial filter temperature and accumulated soot distribution at the onset of the regeneration process (at the so called *balance point*), which has a significant effect on the subsequent temperature evolution in the filter, could not be taken physically plausible into account.

In what follows, the basic tools to analyse on a purely theoretical basis physical and chemical phenomena in DPFs are presented.

OpenFOAM

OpenFOAM is a C++ library, used primarily to create executables, known as applications. The applications fall into two categories: solvers, that are each designed to solve a specific problem in continuum mechanics; and utilities, that are designed to perform tasks that involve data manipulation. The OpenFOAM distribution contains numerous solvers and utilities covering a wide range of problems [18].

One of the strengths of OpenFOAM is that new solvers and utilities can be created by its users with some pre-requisite knowledge of the underlying method, physics and programming techniques involved [17].

For all the above reasons, OpenFOAM is the perfect basis for a multiscale, multiphysics software tool that can be used for exhaust gas aftertreatment development.

DexaSIM

In the past extensive research and software development on Diesel exhaust system modelling has already been performed The result is the software called Diesel EXhaust gas Aftertreatment SIMulation, in short: DexaSIM [3, 4, 9, 12, 15, 23, 24, 25, 27, 28, 29]. DexaSIM in its current experimentally validated development status permits the simulation of filter loading due to soot deposition on a microscopic material level and globally in the exhaust system. In the latter case also heat conduction processes in the solid filter material can be taken into account. Additionally chemical reaction schemes to model filter regeneration on a microscopic and macroscopic level are already integrated. An overview of DexaSIM and all its multiscale, multiphysics [14, 29] modules is shown in Figure 1. Highlighted are the modules that are important for the multiscale approach.

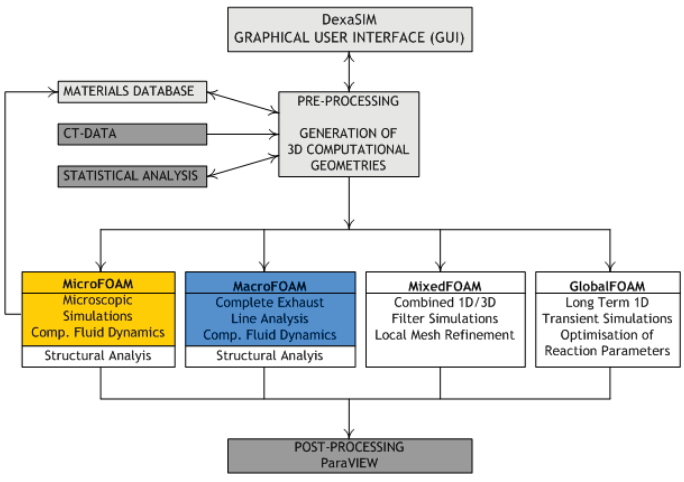

Figure 1 General structure of DexaSIM, highlighted are the multiscale modules

Computational Fluid Dynamics (CFD) in the microstructures based on the Open Source software OpenFoam [31] is used to bridge the gap between the materials microscopic structure and the macroscopic properties needed in the global analysis of the complete exhaust system.

The microstructural CFD module MicroFOAM computes the permeability of clean and soot loaded filter material samples. The global permeability data as a function of soot loading are stored in a database and can be subsequently accessed by the module MacroFOAM, which enables the analysis of the complete exhaust systems. In both software modules modelling of soot particle flow and deposition is based on the Method-of-Moments [28].

By using this approach of combining the flexibility of OpenFOAM and the GUI of DexaSIM, multiscale simulation methods are embedded in one single program system, whereby the visualisation of all computed results is done via the Open Source Post-Processing software ParaView [32].

Modelling on a microscopic scale

The microstructural geometry generator contained within DexaSIM permits the reconstruction of material samples from 2D Computer Tomography (CT) data and from 2D Scanning Electron Microscopy (SEM) data. By using statistical functions (e.g. pore diameter distribution, pore distance autocorrelations, lineal path functions, etc.) material samples are mathematically characterised. These data are stored in a database (see Figure 1) and can be retrieved to change or modify via variation of mathematical parameters a certain material sample and to design new materials with improved performance. Additionally via clustering/filtering of CT grey scale images, deposited soot or accumulated ashes can be detected [4].

Isotropic material reconstruction method

The reconstruction of an isotropic digitised model (mesh) of any porous structure can be summarised by the following steps:

1. obtaining a 2D digital image of the material
2. retrieving statistic parameters of the image using DexaSIM [2, 6, 22, 26, 33]
3. reconstruct 3D digital model or mesh according to statistical parameters [1, 8]

An example of the reconstruction of a foam structure from a 2D CT image can be seen in Figure 2.

The previous described algorithm creates a 3D computational model out of a 2D image. This always returns an isotropic computational model with the same statistical characteristics in all main directions.

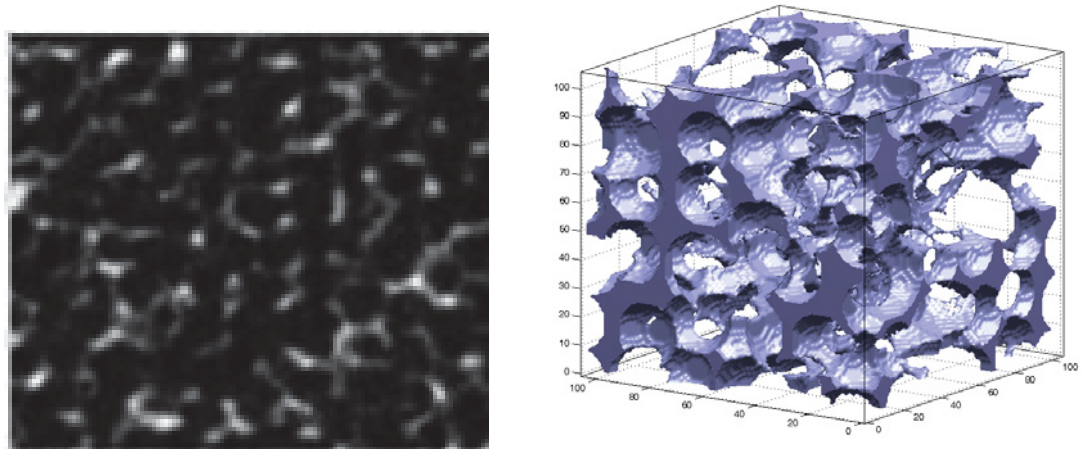

Figure 2 Computer Tomography (CT) image of a foam material (left) and the computational model of the foam material after reconstruction (right).

Anisotropic material reconstruction method

The algorithm used to digitise 2D CT-scans can also be expanded in the third dimension to create anisotropic (real) 3D computational models of any material. The algorithm then includes the following steps:

1. Obtain 2D grey-scale images of the material
2. Combine 2D images to one 3D grey-scale image
3. Digitise and reconstruct the 3D digital model or mesh

An example of the reconstruction of a 3D CT image of an anisotropic structure is shown in Figure 3.

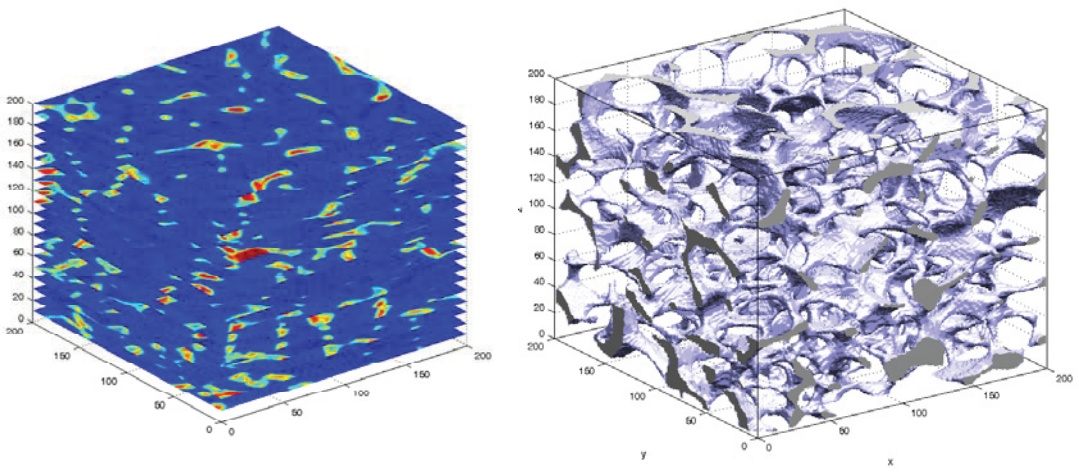

Figure 3 Computational model (right) of a 3D CT-scan (left) of a foam structured material

Microscopic simulations

From the 2D CT scan of filter material as shown in Figure 2, a 3D computational foam model has been created. From this 3D model, different models are generated by either eroding or adding filter material in order to change the porosity (see Figure 4). On these models, the influence of the initial porosity on the permeability and the influence of soot deposition inside the foam structure have been investigated.

Geometries

Based on one typical CT image of a DPF filter, a 3D computational model of a cube (side length 5.3mm) is created (Cube2). The production process of foam filters allows creating different porosities from the same material based on the production speed and amount of gas used during the production process. In order to simulate this influence, two more models are created from Cube2 by eroding and by uniformly filling the model Cube2. This way, respectively a model with a higher porosity (Cube3) and a lower porosity (Cube1) results (Figure 4).

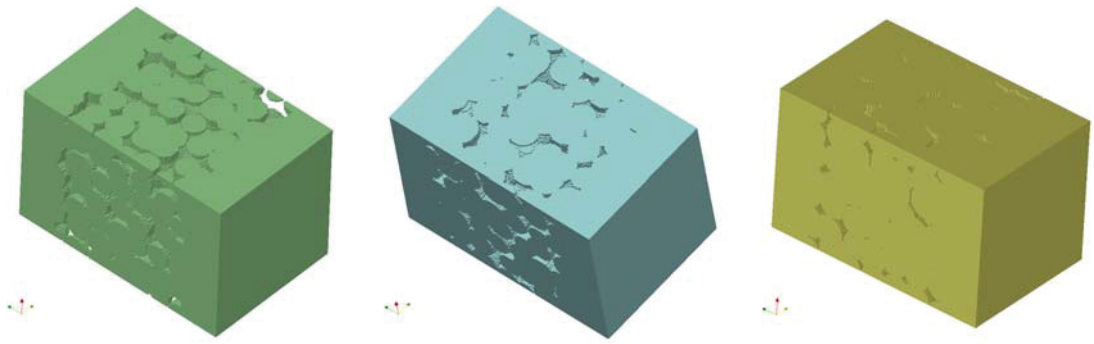

Figure 4 Computational 3D models of three cubes: Cube1 (left), Cube2 (middle) and Cube3 (right). The fluid zone is shown.

Cube2 contains a voxel based mesh of uniform sized hexahedral cells, created by DexaSIM. The automatic mesh generator SPIDER [30] has also been used to create a body fitted mesh for the geometry of Cube2; once with 350.000 cells (Cube2_spider_350k) and once with 1.500.000 cells (Cube2_spider_1500k). The meshes generated this way have smoother pore walls. This is shown in Figure 5.

SPIDER can not yet handle periodic boundary conditions. For this reason, another model of Cube2 has been created Cube2_wall, with walls instead of periodic boundary conditions. Table 1 shows the amount and type of cells in the created models.

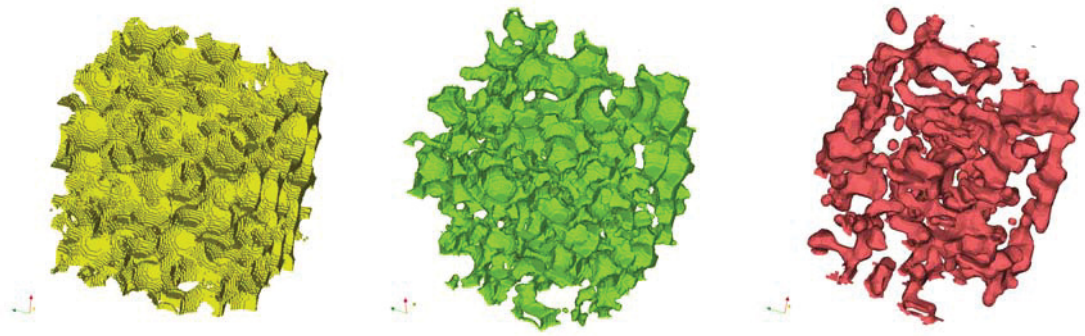

Figure 5 Comparison of pore walls fort he Cube2 model, created with DexaSIM (left) and SPIDER with 350.000 cells (right) and 1.500.000 cells (middle).

Boundary conditions

All models were simulated by defining a fixed pressure drop between inlet and outlet. Both the inlet and outlet region were elongated for simulation stability reasons. The side walls are periodic boundaries, except for the SPIDER models where the side walls are walls. The pore walls are set to walls as well (Table 1).

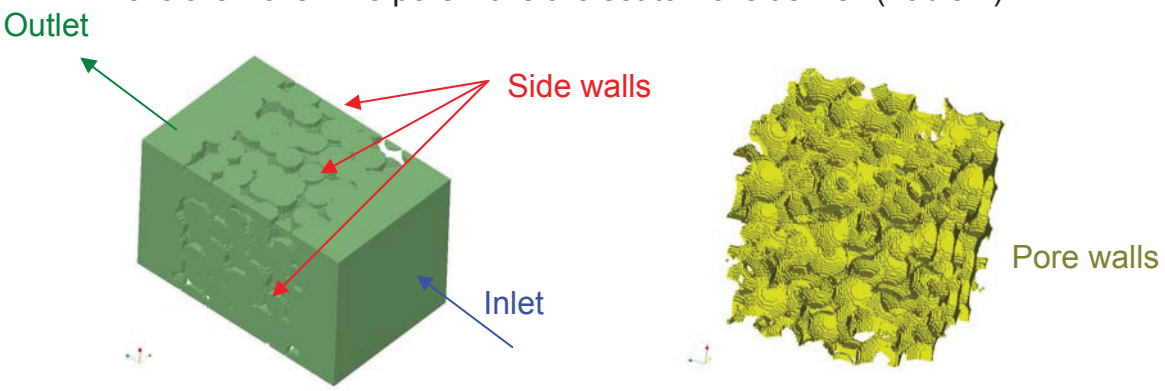

Table 1 Cell information and boundary conditions used for the models

Model	Cells		Boundary Conditions			
Cube1	Number	Type	**Inlet**	**Outlet**	**Side walls**	**Pore walls**
Cube1	1.450.000	Hexahedra	Pressure	Pressure	Periodic	Wall
Cube2	1.670.000	Hexahedra	Pressure	Pressure	Periodic	Wall
Cube3	1.820.000	Hexahedra	Pressure	Pressure	Periodic	Wall
Cube2_wall	1.670.000	Hexahedra	Pressure	Pressure	Wall	Wall
Cube2_spider_350k	350.000	Mixed	Pressure	Pressure	Wall	Wall
Cube2_spider_1500k	1.500.000	Mixed	Pressure	Pressure	Wall	Wall

Permeability

The permeability of the digitized foam structures is calculated from plotting the pressure drop for different mass flows through the model. The calculations are done using OpenFOAM and DexaSIM.

The OpenFOAM solver used is a steady state solver specialised for filter simulations developed by ICE Strömungsforschung GmbH and is called steadyFilterFoam [29].

The three cubes with different porosity show clear differences in pressure drop for different mass flows. The difference between periodic (Cube2) and wall boundary conditions (Cube2_wall) can be seen in Figure 9. The influence of a too coarse mesh (Cube2_spider_350k) and the difference between a voxel mesh and a body fitted mesh (Cube2 and Cube2_spider_1500k, Figure 11).

The voxel based meshes show a higher pressure drop. The pore walls are not smooth but show a highly cubic pattern. This raises the flow resistance and hence increases the pressure drop over the model. However, the smoothening of the side walls by SPIDER in order to create a body fitted mesh causes a change in solid and hence fluid volume (Figure 6).

A solid model that has a convex dominated structure will gain fluid volume and hence its porosity will increase and vice versa for a concave dominated structure (Figure 7). The porosity and fluid volume have been calculated for all volumes and are illustrated in Table 2. It can be concluded that Cube2 is a convex dominated structure.

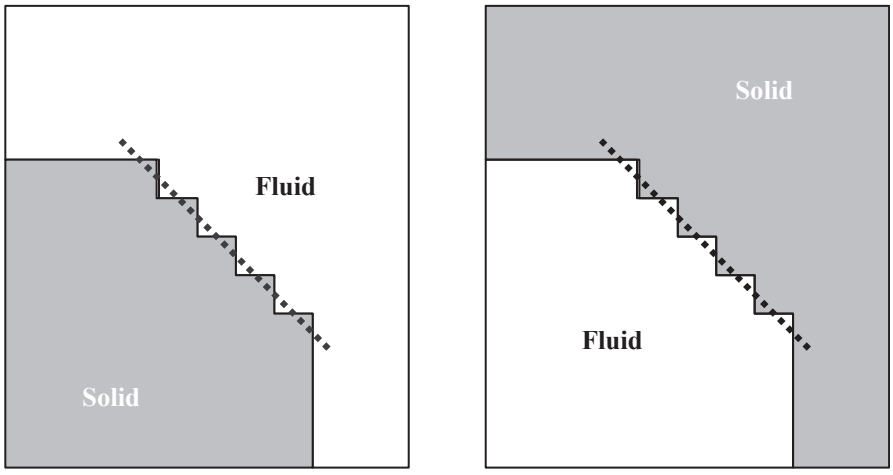

Figure 6 Illustration of how the automatic mesh generator SPIDER smoothens convex and/or concave walls.

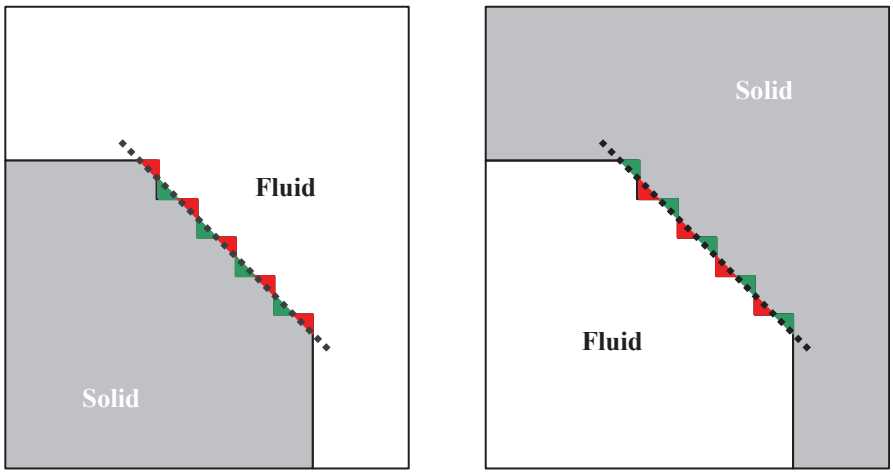

Figure 7 Change in solid volume (red triangles are deleted and green triangles are created) due to automatic mesh generation by SPIDER for a convex (left) and concave (right) solid volume

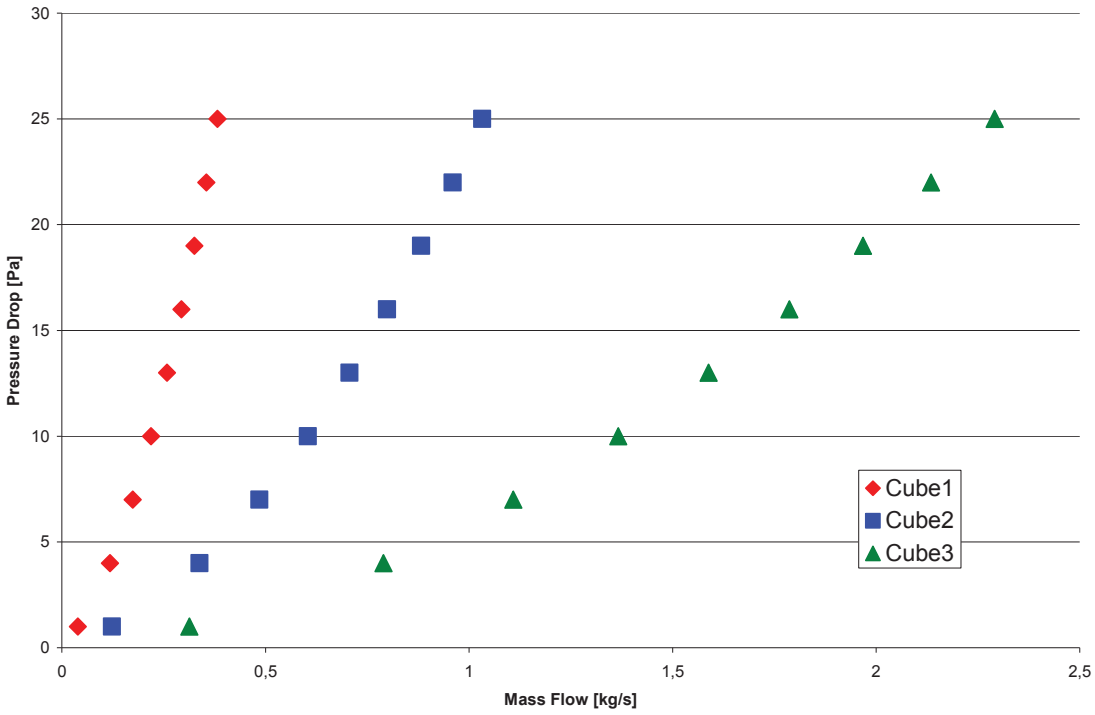

Figure 8 Pressure drop vs. Mass flow for the three cube models

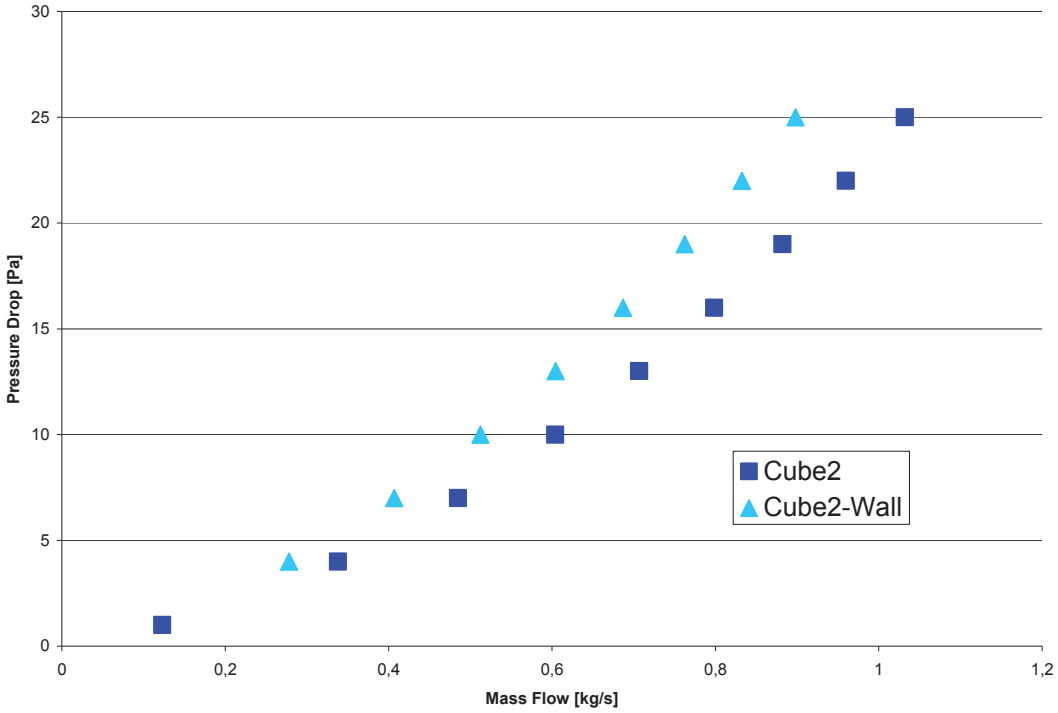

Figure 9 Pressure drop vs. Mass flow for the different boundary conditions at the side walls

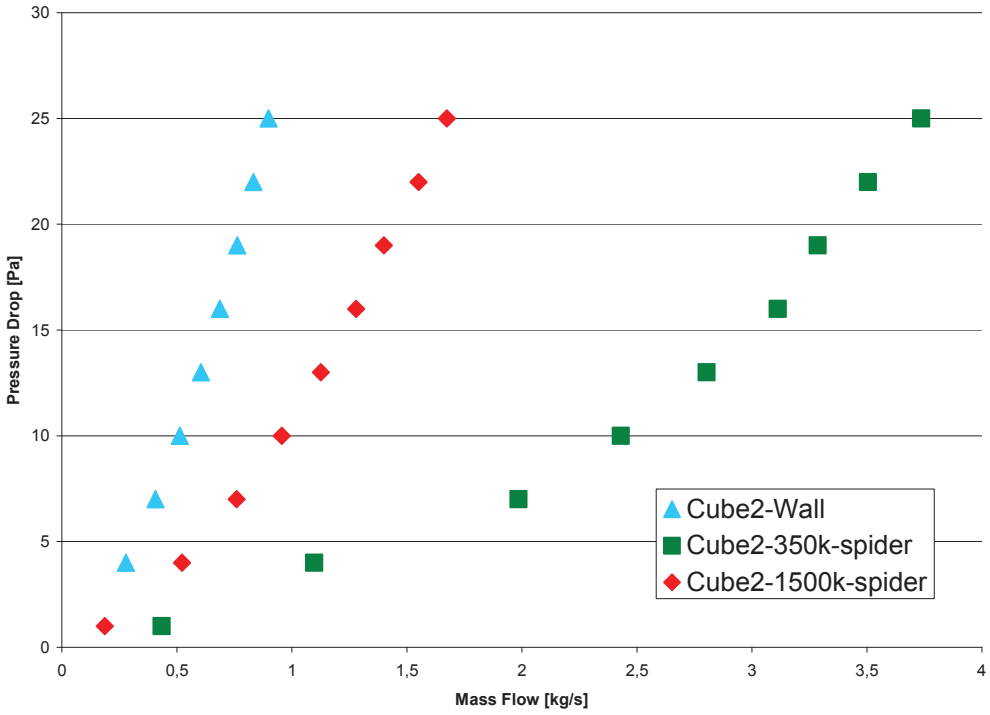

Figure 10 Comparison between the pressure drop for the voxel based mesh (Cube2_wall) and the body fitted mesh (SPIDER)

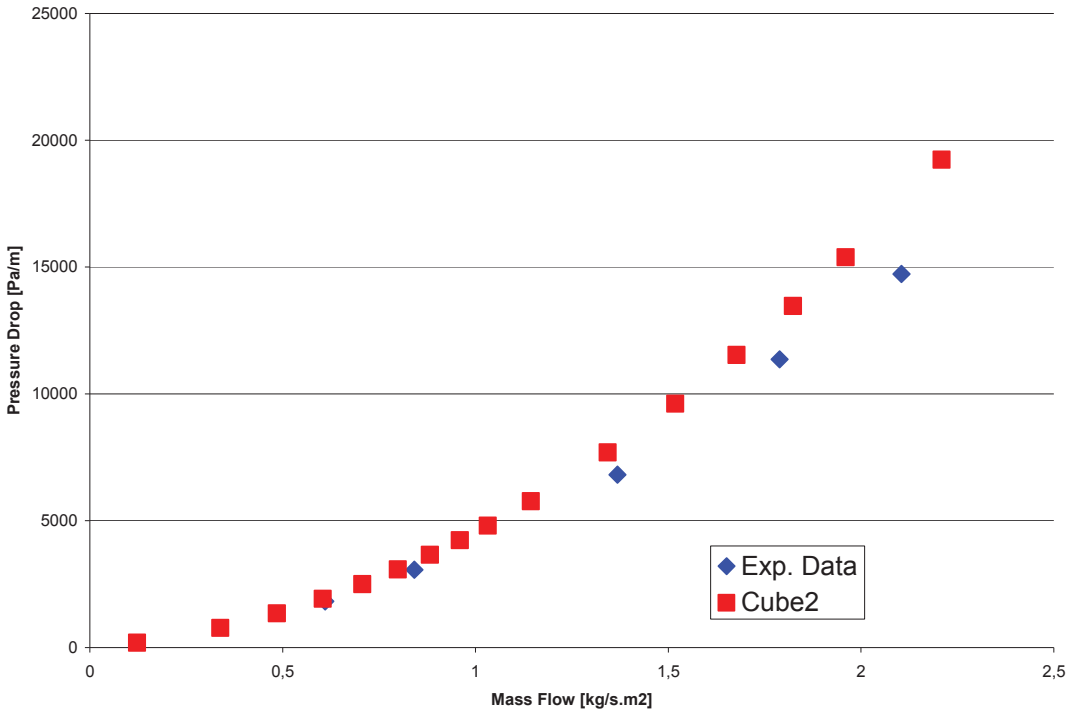

Figure 11 Comparison between simulation (Cube2) and experiment

The following relation exists between the pressure drop and the velocity (density = 1.18kg/m3):

$$\Delta P = \frac{\mu}{C_1} L \cdot v + \frac{\rho \cdot \mu}{C_2} L \cdot v^2$$

With

Δp	Pressure drop			
μ	Gas viscosity	=	1.5e-5	Pa.s
L	Model length	=	5.3e-3	m
ρ	Gas density	=	1.18	Kg/m^3
C_1	Permeability * L			
C_2	Forchheimer term			

Table 2 shows the calculated values of C_1 and C_2 for all models.

Table 2 Results on permeability for all models

Model	Fluid volume [m^3]	Porosity	Specific. Surface [m^2/m^3]	C_1 [m^2]	C_2 [m]
Cube1	1.75e-7	0.64	4111	4,046e-8	0,0051
Cube2	1.94e-7	0.77	3639	1,362e-7	0,0342
Cube3	2.11e-7	0.88	2569	3,927e-7	0,1571
Cube2_wall	1.94e-7	0.77		9,323e-8	0,0283
Cube2_spider_350k	2.12e-7	0.89		2,750e-6	0,3679
Cube2_spider_1500k	2.00e-7	0.81		1,752e-7	0,0973

The porosity is defined as the ratio between the volume in the pores (fluid zone) and the total volume of the cube. The specific surface is defined as the total surface area per unit of solid or bulk volume.

Soot deposition

The soot deposition on a microscopic structure has been simulated using Cube2 with periodic boundary conditions and using a transient solver. The soot deposition at the pore walls has been simulated by introducing a source term (S_{soot}) in the soot transport equation. The soot term can be written as

$$S_{soot} = R_{dep}\alpha\rho_{soot} \quad 1.$$

where α defines the ratio of the cell surface at the wall to the complete cell volume (Figure 12) and determines the amount of soot present in that cell that can be deposited relative to the wall surface. R_{dep} is the deposition rate in that cell, depending on the local flow velocity averaged over the cell. This source term defines the amount of free flowing soot that is being deposited at the pore wall. The transport equation for the soot in the fluid flow (2.) and the deposited soot (3.) can be written as

$$\frac{\partial\rho_{soot}}{\partial t} + \nabla\cdot u\rho_{soot} - \nabla\cdot K\nabla\rho_{soot} + S_{soot} = 0 \quad 2.$$

$$\frac{\partial\rho_{dep}}{\partial t} - S_{soot} = 0 \quad 3.$$

Where

ρ_{soot}	Soot density
u	Soot velocity
K	Soot diffusion
α	Ratio of wall surface in cell to cell volume
v_{dep}	Soot diffusion

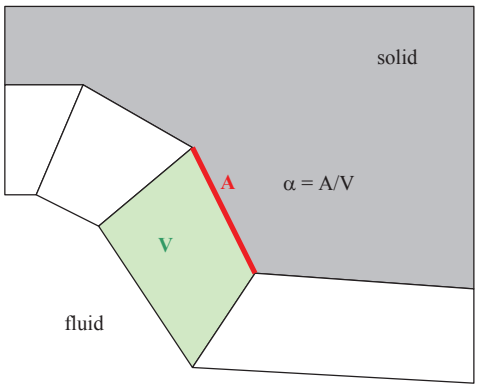

Figure 12 Definition of the surface to volume ratio a that defines the deposition speed.

At the same time, a scalar called the *depot ratio D* is introduced in the pressure-velocity momentum equation that defines the ratio of the soot volume to the total volume in that cell. This scalar is multiplied by a constant resistance *R*, so that the resistance gradually rises with the filling of a cell with soot (A, B in Figure 13). As soon as the cell is completely filled, the resistance is maximum, or the porosity falls to zero (C). At this point, the cell is taken out of the fluid zone and added to the solid zone (D).

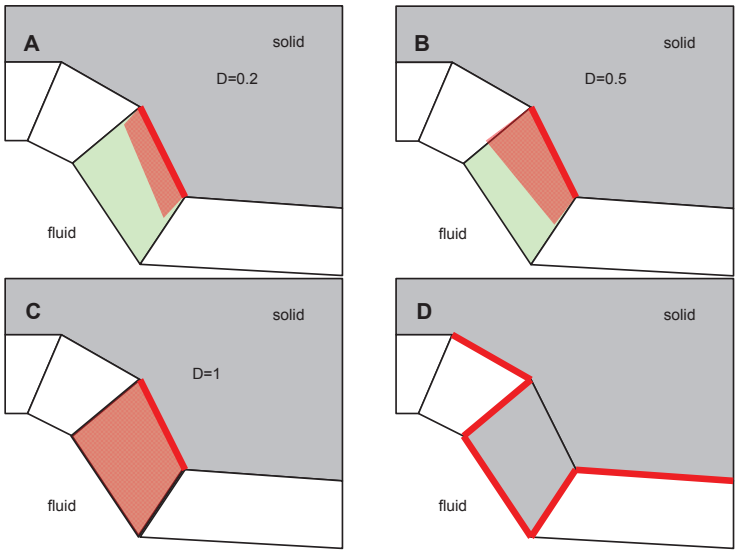

Figure 13 Filling of a cell with soot causes the depot ratio D to rise to a maximum (A, B, C) after which the cell is taken out of the fluid zone (D).

Figure 14 shows the change in resistivity (1/permeability) due to the filling of the pores in Cube2. After about 10% of the pore space is filled, the resistivity rises stronger than linear which has its influence on the flow pattern through the structure (Figure 15).

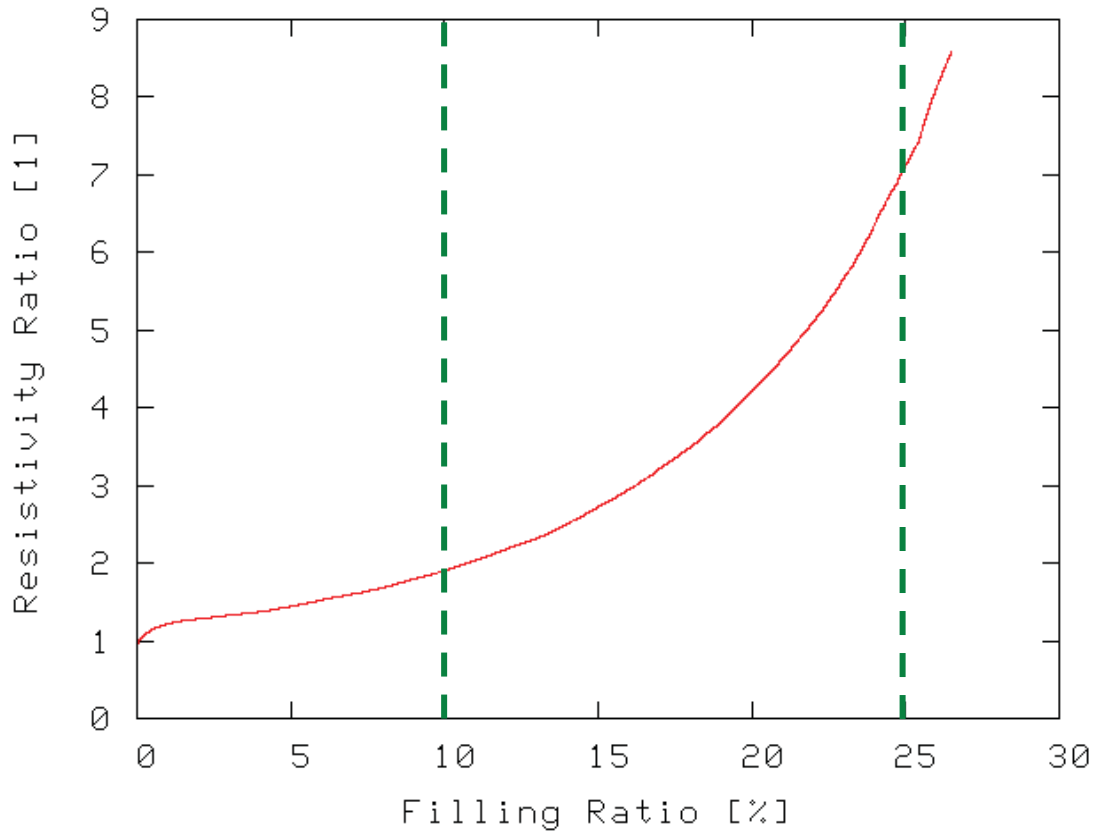

Figure 14 Change in resistivity due to the filling of the pores with soot.

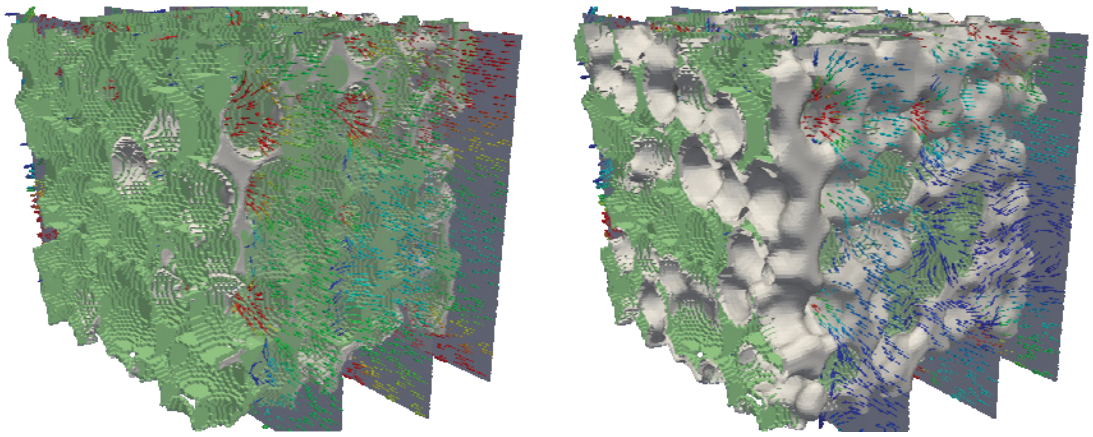

Figure 15 Illustration of a microscopic pore structure (green) that is gradually being filled with soot (grey): 10% (left) and 25% (right). On three surfaces, velocity magnitude vector plots are shown.

Macroscopic simulations

Using the results and material parameters obtained from the microscopic simulations on Cube2, a macroscopic simulation on a simple fictive exhaust system has been conducted. The exhaust system has been setup using DexaSIM (Figure 16) and it consists of two filters. The first filter takes care of the oxidation of CO and NO. The second filter is a passive soot trap. Some results are plotted in Figure 17.

The chemistry simulated is a simplified Continuous Regeneration Trap (CRT). The simplified reaction scheme is:

$$\begin{aligned} 2CO + O_2 &\rightarrow 2CO_2 \\ 2C_2H_6 + 7O_2 &\rightarrow 4CO_2 + 6H_2O \\ 2NO + 2CO &\rightarrow N_2 + 2CO_2 \end{aligned} \qquad (4.)$$

This reaction scheme is just an example. Both OpenFOAM and DexaSIM use CHEMKIN [34] files to describe the chemical reactions inside the model, which allows the programs to simulate any chemical reaction.

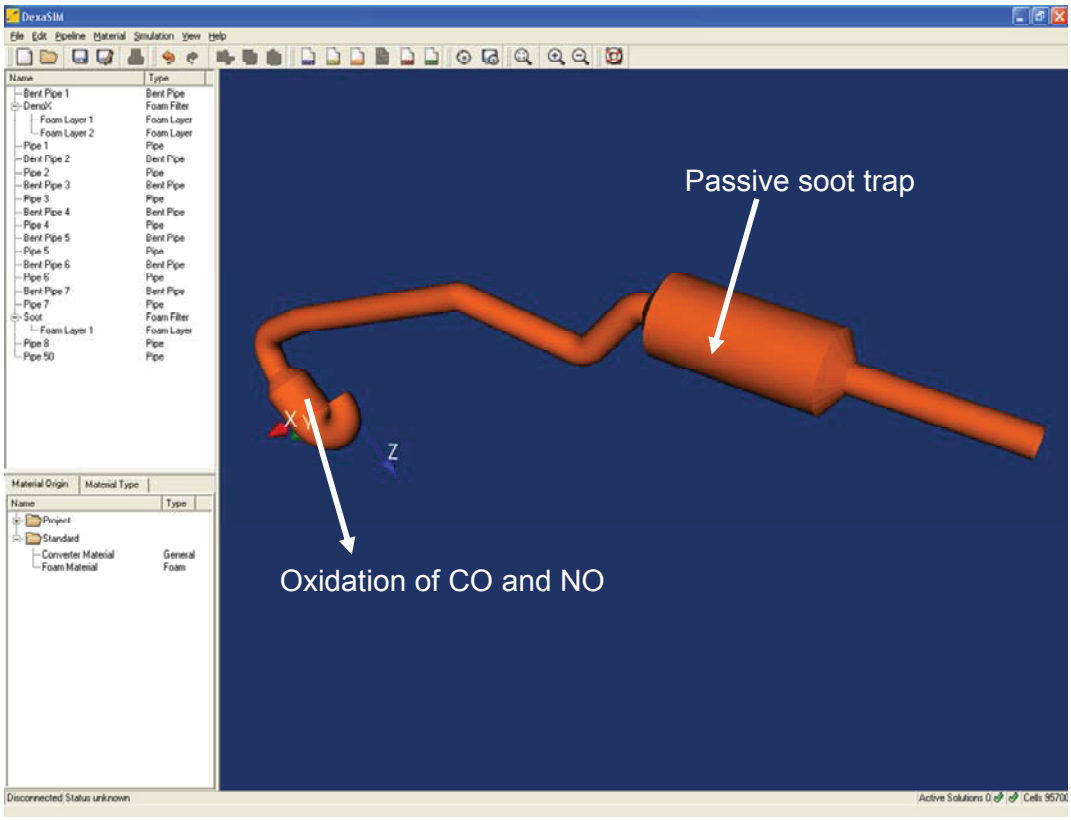

Figure 16 Setup of simple exhaust system using DexaSIM

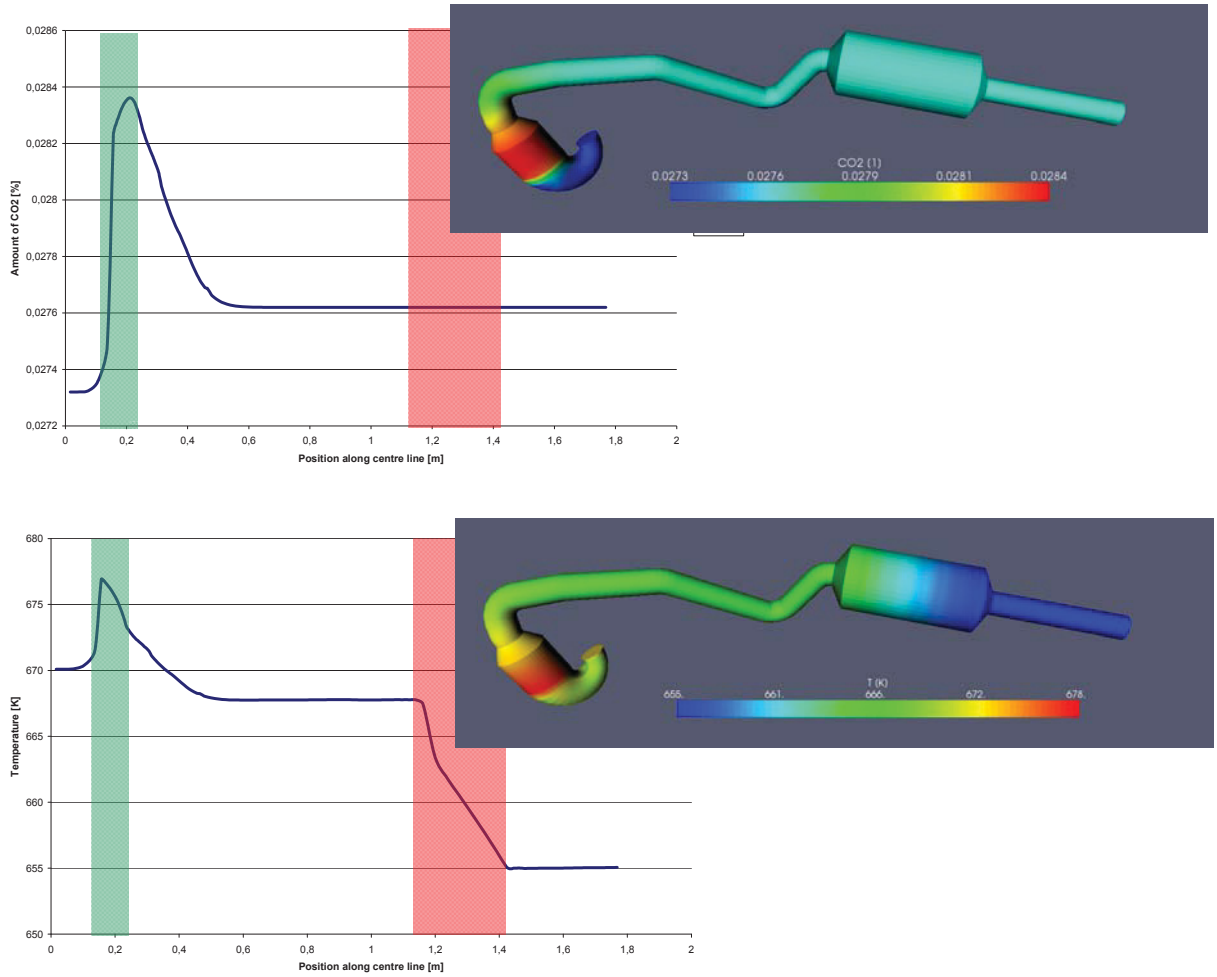

Figure 17 Contour plots and data plot along centre line fort he CO2 concentration (top) and the temperature (bottom). The position of the filters is indicated by the green (oxidation) and red (soot) areas.

Conclusion

The modelling approach described above builds on the multiscale link between microstructural evolution and specific macroscopic exhaust system features with the objective to achieve major improvements in material design. A complete method has been presented to study filter materials on a microscopic level to see the influence of microscopic design and optimization on the macroscopic filter behaviour.

OpenFOAM offers the possibility of combining microscopic and macroscopic scale simulations in one tool, i.e. DexaSIM. The first validations of the simulations with experimental results look promising. The combination of a microscopic and macroscopic tool leads to a better understanding of the product and shows where the optimization potential is.

An outlook for the created method would comprise extensive experimental validating of the models, the implementation of submodels for the wall flow filter (anisotropic approach) and submodels for thermal activity inside the filter material (thermal tension, cracking, fluid-structure coupling).

Acknowledgements

Our work in this area has been supported by the European Union (EU) through the FP5 projects SYLOC-DEXA (G3RD-CT-1999-00014), STYFF-DEXA (G3RD-CT2002-00785) and IMITEC (IST–2001-34874), our partners in the DEXA cluster and Mr. Ferdinand Kickiger for allowing us to use his automatic mesh generator SPIDER.

Bibliography

[1] Bach, G., *Über die Bestimmung von charakteristischen Größen einer Kugelverteilung aus der Verteilung der Schnittkreise*, Zeitschrift für wissenschaftliche Mikroskopie **65**,1963, pp. 285-291

[2] Borgefors, G., Nyström, I., *Efficient shape representation by minimizing the set of centres of maximal discs/spheres*, Pattern Recognition Letters, Vol. **18**, 1996, pp. 465-472

[3] Brandstätter, W., Wassermayr, C., Prenninger, P., *An Integrated Approach for the Design of Diesel Engine Exhaust Systems to meet Euro 4 and beyond Emissions Legislations*, THIESEL 2002/Thermodynamic Processes in Diesel Engines, 11.-13. September 2002, Valencia

[4] Brandstätter, W., Leixnering, J., Faraldi, P., Merlone Borla, E., Ranalli, M., Vlachos, N., Konstandopoulos, A.G., *The STYFF-DEXA Project: Advanced Simulation Tools for Ceramic Foam Diesel Particulate Filters*, ICE2005 - 7th International Conference on Engines for Automobile 11/09/2005 - 16/09/2005

[5] Brandstätter, W., Leixnering, J., Faraldi, P., Ranalli, M. and Vlachos, N., *The STYFF-DEXA Project: Advanced Simulation Tools for Ceramic Foam Diesel Particulate Filters*

[6] Breu, H., Gil, J., Kirkpatrick, D., and Werman, M., *Linear Time Euclidean Distance Transform Algorithms*, IEEE Transactions on Pattern Analysis and Machine Intelligence, Vol. **17**, No. 5,1995, pp. 529-533

[7] DexaSIM User manual, DexaSIM 0.9, ICE Strömungsforschung GmbH, 2007

[8] Goldsmith, P.L., The calculation of true particle size distribution from the sizes observed in a thin slice, Brit. J. Appl. Phys. **18**, 1967, pp. 813-830

[9] Gschaider, B.F.W., Honeger, C.C., Redl, C.E.P, *Soot Particle Deposition within Porous Structures Using a Method of Moments Lattice Boltzmann Approach*, Computational Science ICCS 2004, 4th International Conference Krakòw Poland, June 6-9, 2004

[10] Gschaider, B.F.W., Honeger, C.C., Redl, C.E.P., *Soot Particle Deposition within Porous Structures Using a Method of Moments*, Lattice Boltzmann

Approach, Computational Science ICCS 2004 4th International Conference Krakòw Poland, June 6-9, 2004

[11] Janoske, U., Deuschle, T., Piesche, M., *Modelling of Filtration and Regeneration Processes in Diesel Particulate Traps*, Mathematics in Industry, Vol. **8** Progress in Industrial Mathematics at ECMI 2004, part III, pp 252-256 Springer Berlin Heidelberg, 2006

[12] Konstandopoulos et al., *The Diesel Exhaust Aftertreatment (DEXA) Cluster: A Systematic Approach to Diesel Particulate Emission Control in Europe*, A.G., SAE 2004-01-0694

[13] Kostoglou, M., Housiada, P., Konstandopoulos, A.G., (2003), *Multi-channel simulation of regeneration in honeycomb monolithic diesel particulate filters*, Chemical Engineering Science, **58**, pp. 3273-3283.

[14] Mataln, M., Brandstätter, W., *A Unified Approach to Model Fluid-Structure Interactions,* Petroleum Engineering Seminar 2005, University of Leoben

[15] Mohammed, H., Triana, A.P., Johnson, J.H., Yang, S-L., *An Advanced 1D 2-Layer Catalyzed Diesel Particulate Filter Model to Simulate: Filtration by the Wall and Particulate Cake, Oxidation in the Wall and Particulate Cake by NO2 and O2, and Regeneration by Heat Addition* SAE 2006-01-0467

[16] Muntean, G., Rector, D., Herling, D., Khaleel, M., Lessor, D., *Lattice-Boltzmann Diesel Particulate Filter Sub-Grid Modelling-A Progress Report*, SAE 2003-01-0835

[17] OpenFOAM, the Open Source CFD Toolbox, OpenFOAM 1.4.1, Programmer's Guide, OpenCFD Limited, 2007.

[18] OpenFOAM, the Open Source CFD Toolbox, OpenFOAM 1.4.1, User Guide, OpenCFD Limited, 2007.

[19] Potikakis, G., Stamatelos, A., 2006, *Three-Dimensional Catalytic Regeneration Modeling of SiC Diesel Particulate Filters*, Journal of Engineering for Gas Turbines and Power, **128**, pp. 421-433.

[20] Pontikakis, G., Stamatelos, A., *Three-Dimensional Catalytic Regeneration Modeling of SiC Diesel Particulate Filters*, Journal of Engineering for Gas Turbines and Power, April 2006, Vol. **128**, pp 421-433

[21] Press, W.H., Teukolsky, S.A., Vetterling, W.T., Flannery, B.P., *Numerical Recipes in C, The Art of Scientific Computing*, Second Edition, Cambridge University Press, 1992

[22] Ragnemalm, I., *The Euclidean Distance Transform*, Ph.D. Dissertation, 1993, Linköping University, Sweden

[23] Ranalli, M., Kroner, P., Brandstätter, W., *DPF SOOT MAPPING. A Simple and Cost Effective Measurement Method for Series Development*, World Automotive Congress, Barcelona, Spain, May 23-27, 2004

[24] Redl, C., *In situ combustion modeling in porous media using Lattice-Boltzmann methods*, ECMOR VIII/3.-6. September 2002, Freiberg

[25] Redl, C., Wassermayr, C., Leixnering, J., *On The Numerical Simulation in Foam Filter Design For Diesel Exhaust Gas System*, Haus der Technik, Essen 2003

[26] Wai-Pak Choi, Kin-Man Lam, Wan-Chi Siu, *Extraction of the Euclidean skeleton based on a connectivity criterion*, Pattern Recognition, Vol. **36**, 2002, pp. 721-729

[27] Wassermayr, C., Kästenbauer, M., *Modelle zur Berechnung von Strömung in Partikelfiltern*, Forschungsinformationen der Montanuniversität Leoben, 2001

[28] Wassermayr, C., Brandstätter, W., Schreier, H., Prenninger, P., *Virtual Engineering of Diesel Exhaust Systems to Meet Future Emission Legislation*, Presented at 2003 JSAE Annual Congress

[29] www.ice-sf.at

[30] www.meshing.org

[31] www.openfoam.org

[32] www.paraview.org

[33] Yeoung, C.L.Y., and Torquato, S., *Reconstructing random media*, Physical Review E, Vol. **57**, No. 1, 1997, pp. 495-506

[34] http://public.ca.sandia.gov/chemkin//index.html